Nuclear mass predictions of the relativistic continuum Hartree-Bogoliubov theory with the kernel ridge regression

X. H. Wu (吳鑫輝) ,[1,2,*] C. Pan (潘琮),[3] K. Y. Zhang (张开元) ,[4] and J. Hu (胡进) [1]

[1]*Department of Physics, Fuzhou University, Fuzhou 350108, Fujian, China*
[2]*State Key Laboratory of Nuclear Physics and Technology, School of Physics, Peking University, Beijing 100871, China*
[3]*Department of Physics, Anhui Normal University, Wuhu 241000, China*
[4]*Institute of Nuclear Physics and Chemistry, CAEP, Mianyang, Sichuan 621900, China*

Background: Nuclear masses are of fundamental importance in both nuclear physics and astrophysics, and the masses for most neutron-rich exotic nuclei are still beyond the experimental capability. The relativistic continuum Hartree-Bogoliubov (RCHB) theory has achieved great successes in the studies of both stable and exotic nuclei. The mass table based on the RCHB theory has been constructed with the assumption of spherical symmetry [Xia *et al.*, At. Data Nucl. Data Tables **121**, 1 (2018)]. The upgraded version including deformation effects based on the deformed relativistic Hartree-Bogoliubov theory in continuum (DRHBc) is under construction, and the part for even-even nuclei has been finished [Zhang *et al.*, At. Data Nucl. Data Tables **144**, 101488 (2022)]. The kernel ridge regression (KRR) approach is a useful machine-learning approach in refining nuclear mass prediction, and is found to be reliable in avoiding the risk of worsening predictions at large extrapolation distance [Wu and Zhao, Phys. Rev. C **101**, 051301(R) (2020)].

Purpose: The aim of this work is to combine the RCHB mass model and the KRR approach to construct a high-precision and reliable nuclear mass model describing both stable and weakly bound neutron-rich exotic nuclei. Another purpose is to utilize the masses of even-even nuclei from the DRHBc theory to validate the performance of the KRR approach.

Method: The KRR approach is employed to refine the RCHB mass model by learning and representing the mass residual of the RCHB mass model with the experimental data. The leave-one-out cross-validation is applied to determine the hyperparameters in the KRR approach. The DRHBc mass model for even-even nuclei is employed to help to analyze the physical effects included in the KRR corrections and examine the KRR extrapolations.

Results: The refined RCHB mass model with KRR corrections can achieve an accuracy of root-mean-square deviation 385 keV from the experimental masses. The major contributions contained in the KRR corrections are found to be the deformation effects. The KRR corrections also contain some residual deformation effects and some other effects beyond the scope of the DRHBc theory. The extrapolation of the KRR approach in refining the RCHB predictions is found to be very reliable.

Conclusions: A mass model benefiting from the RCHB model with continuum effects properly treated and the KRR approach is constructed. This model is demonstrated to be accurate in reproducing the masses of experimentally known nuclei and reliable in extrapolating to the experimentally unknown neutron-rich regions.

I. INTRODUCTION

Nuclear masses are important for both nuclear physics [1] and astrophysics [2]. They reflect many underlying physical effects of nuclear quantum many-body systems, and can be used to extract nuclear structure information, e.g., nuclear deformation [3], shell effects [4], and nuclear force [5]. They also determine the reaction energies for all nuclear reactions, which are important in understanding the energy production in stars [6] and the study of nucleosynthesis [7–9]. Experimentally, about 2500 nuclear masses have been measured so far [10]. Nevertheless, there are still a large number of nuclei that cannot be accessed experimentally even in the foreseeable future. Theoretically, many models have been applied to predict nuclear masses, including macroscopic models [11], macroscopic-microscopic models [12–15], and microscopic models [16–22]. The macroscopic-microscopic models have achieved good accuracy in reproducing the data of experimentally known nuclei, while the microscopic models are usually believed to have a better reliability of extrapolation [23,24].

Many efforts have been made to predict nuclear masses with microscopic models, such as nonrelativistic and relativistic density functional theories. On the nonrelativistic side, several nuclear mass tables have been constructed based on Hartree-Fock-Bogoliubov calculations with Skyrme or Gogny functionals [17,18,25]. The relativistic theory, i.e., covariant density functional theory (CDFT), has gained wide attention in recent decades for many attractive advantages, such as the

*wuxinhui@fzu.edu.cn

automatic inclusion of the nucleonic spin degree of freedom and the spin-orbital interaction [26], the explanation of the pseudospin symmetry in nucleon spectrum [27–31] and the spin symmetry in antinucleon spectrum [31–33], and the natural inclusion of the nuclear magnetism [34]. The CDFT has proven to be a powerful tool to describe a variety of nuclear phenomena [35–43].

For exotic nuclei which are far away from stability valley and weakly bound, the Fermi energy is very close to the continuum threshold. The pairing interaction can scatter nucleons from bound states to the resonant ones in the continuum, and the density could become more diffuse due to this coupling to the continuum. Therefore, pairing correlations and continuum effects are important for not only the description of exotic nuclei but also the prediction of drip-line locations. This is important for the studies of r process in extremely high neutron density environment, e.g., the neutron star mergers. Based on the CDFT, the relativistic continuum Hartree-Bogoliubov (RCHB) theory, with the pairing correlations and continuum effects properly treated, has been developed [44,45]. The RCHB theory has achieved great successes in the studies of both stable and exotic nuclei [20,46–56]. Based on the RCHB theory and the density functional PC-PK1 [57], the first nuclear mass table including continuum effects has been constructed and the importance of continuum effects on the limits of the nuclear landscape has been discussed [20]. However, limited to the assumption of spherical symmetry, the root mean square (rms) deviation of the RCHB mass table with respect to available data is 7.96 MeV. In order to improve the description of nuclear masses starting from the RCHB model, on the one hand, construction of an upgraded version of the mass table including the deformation and continuum effects simultaneously by using the deformed relativistic Hartree-Bogoliubov theory in continuum (DRHBc) [58,59] is in progress [60–62], and the part for even-even nuclei has been finished [22]. On the other hand, one may improve the predictions of the RCHB mass model with the help of machine-learning approaches.

Recently, machine-learning approaches have been widely employed in nuclear physics [63–66], including the successful and wide applications in refining the predictions of nuclear masses [67–71]. Among the various machine-learning applications in nuclear masses, the kernel ridge regression (KRR) approach is found to be a reliable approach in avoiding the risk of worsening the predictions at large extrapolation [67,72–75], and has been examined to have the ability of assessing known physical effects contained in the RCHB model [76]. This is important for the predictions of exotic nuclei far away from the stability valley. Therefore, the KRR approach is promising to improve the predictions of the RCHB mass model.

In this work, the KRR approach and the RCHB mass model are combined to construct a high-precision nuclear mass table to reliably describe the exotic nuclei far away from the stability valley. The KRR corrections on the RCHB masses are compared with the DRHBc corrections to analyze the physical effects included in the KRR corrections. The KRR extrapolations are examined by taking the DRHBc masses as

pseudoexperimental data beyond the experimentally known region.

II. THEORETICAL FRAMEWORK

The KRR approach is employed to refine the RCHB model, by learning and predicting the mass residuals of the RCHB predictions with the experimental data [10]. The mass residual of the nucleus (Z_i, N_i) is expressed as

$$M_{\text{res}}^{\text{KRR}}(Z_i, N_i) = \sum_{j=1}^{m} K[(Z_i, N_i), (Z_j, N_j)]\alpha_j, \quad (1)$$

where m is the number of nuclei in the training set, α_j are weights to be determined, and $K[(Z_i, N_i), (Z_j, N_j)]$ is the Gaussian kernel function taken as

$$K[(Z_i, N_i), (Z_j, N_j)] = \exp\left[-\frac{(Z_i - Z_j)^2 + (N_i - N_j)^2}{2\sigma^2}\right]. \quad (2)$$

The Gaussian kernel has been validated to have better performance than other kernels, e.g., Laplacian, Matern, Cachy, multiquadric ones, in the nuclear mass predictions [75]. The weights α_j are determined by minimizing the loss function defined as

$$L(\boldsymbol{\alpha}) = \sum_{i=1}^{m} \left[M_{\text{res}}^{\text{KRR}}(Z_i, N_i) - M_{\text{res}}^{\text{Data}}(Z_i, N_i)\right]^2 + \lambda||\boldsymbol{\alpha}||^2, \quad (3)$$

which yields

$$\boldsymbol{\alpha} = (\boldsymbol{K} + \lambda\boldsymbol{I})^{-1}\boldsymbol{M}_{\text{res}}^{\text{Data}}. \quad (4)$$

The σ in kernel function (2) defines the length scale that the kernel affects, and the length scales in the neutron and proton directions are assumed to be the same, i.e., only one σ is introduced in Eq. (2). The λ in loss function (3) determines the regularization strength. Both σ and λ are hyperparameters to be determined by validation procedure.

III. NUMERICAL DETAILS

In the training process of the KRR network, the experimental masses are taken from the AME2020 [10], and the theoretical masses are taken from the RCHB mass table [20]. Their overlap includes 2278 nuclei. The mass data from the DRHBc mass table [22] are taken for comparison, which includes 2886 even-even nuclei, and the overlap with AME2020 includes 603 nuclei.

The hyperparameters (σ, λ) are determined by the leave-one-out cross validation. With a given set of hyperparameters (σ, λ), the refined RCHB results with the KRR correction for each of the 2278 nuclei can be obtained with the KRR network trained on all other 2277 nuclei and the rms deviation can be calculated. The rms deviations obtained by the leave-one-out cross-validation are illustrated in Fig. 1. One can see that the hyperparameters can be well determined according to the minima of the rms deviations. The resultant hyperparameters are $(\sigma = 3.1, \lambda = 0.005)$, and the corresponding rms deviation is 385 keV. The obtained rms deviation 385 keV from the leave-one-out cross-validation can be regarded as the accuracy
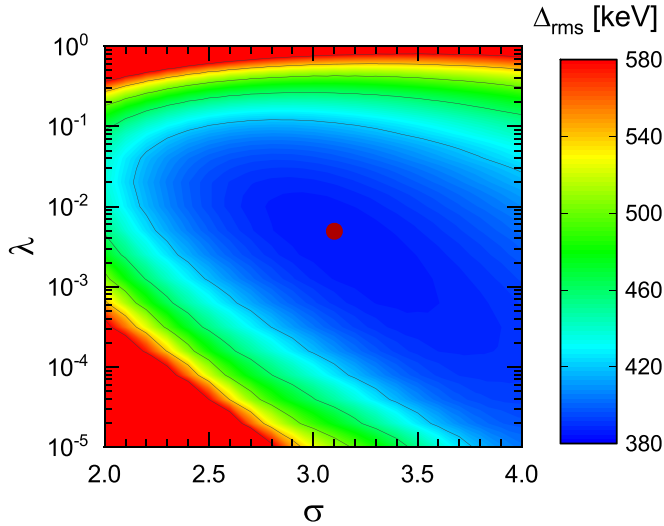
FIG. 1. The rms deviations obtained by the leave-one-out cross-validation with different hyperparameters.

of the KRR predictions on the known experimental data. With the optimal hyperparameters, a refined RCHB mass table with KRR corrections can be built.

IV. RESULTS AND DISCUSSION

The mass deviations of the RCHB [20], DRHBc [22], and KRR predictions with the experimental data AME2020 are presented in Fig. 2. As can be seen, the RCHB predictions reproduce the masses of spherical nuclei around the magic number very well, but the deviations are large when referring to open-shell nuclei due to the assumed spherical symmetry in the RCHB theory. Note that, the masses near $N = 126$ are overestimated by the RCHB calculation, showing that the shell effects here are overestimated.

Both the inclusion of deformation effects in the DRHBc calculations and the inclusion of KRR corrections can improve the RCHB predictions. By comparing the DRHBc and RCHB results, it is found that the deformation effects significantly improve the descriptions of masses, especially for the nuclei with the neutron number between two magic numbers,
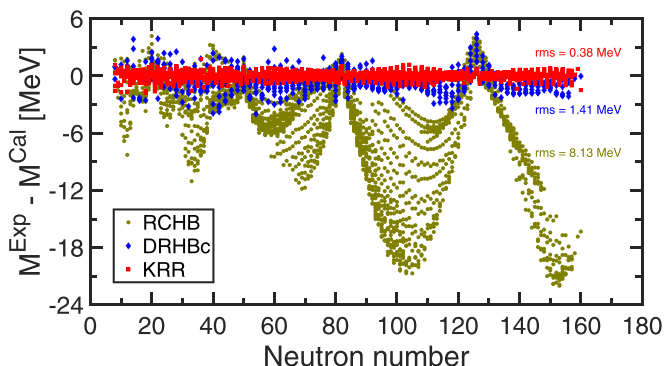

FIG. 2. The mass deviations of the RCHB [20], DRHBc [22], and KRR predictions with the experimental data AME2020.
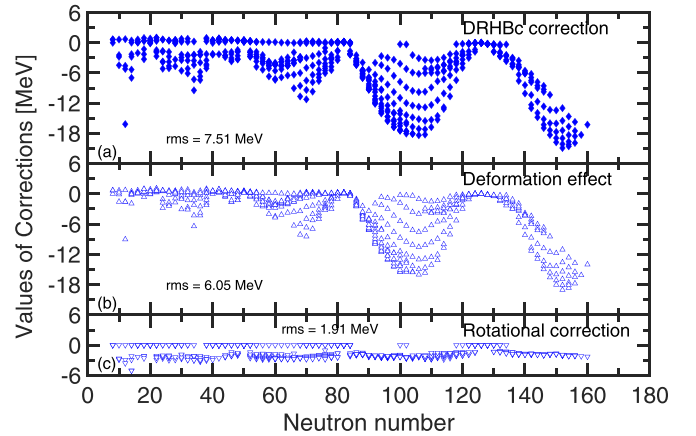

FIG. 3. (a) The full DRHBc corrections on the RCHB predictions. (b) The DRHBc corrections from the deformation corrections of the intrinsic mean field. (c) The DRHBc corrections from the rotational corrections from the beyond mean-field effects.

and the rms deviation is reduced to 1.41 MeV. It is also noted that for some nuclei the deviation from data is still considerable, such as the parabolic behavior near $N = 60$, which may correspond to some residual deformation effects that are not fully considered in the framework of DRHBc. The overestimation near $N = 126$ still remains in the DRHBc predictions. With the KRR corrections, it is found that the deviations are generally small, and the rms deviation is remarkably reduced to 0.38 MeV. The parabolic behavior near $N = 60$ and the overestimation around $N = 126$ are both eliminated by the KRR corrections, showing that the KRR network captures the correct physical effects for both of them. The residual small deviations could come from the residuals of some known effects, and may also come from several sophisticated unknown physical effects.

Since both the DRHBc model with deformation effects and the KRR model show significant improvement in comparison with the RCHB model, it would be interesting to extract and compare their corresponding corrections on nuclear masses. The detailed illustrations are presented in Figs. 3 and 4. The DRHBc correction here in Fig. 3(a) is defined as the deviation of the DRHBc predictions with the RCHB ones. According to the discussion in Ref. [22], the DRHBc corrections can be divided into two parts, i.e., the deformation corrections at the mean-field level, and the rotational corrections from the beyond mean-field effects. As can be seen in Fig. 3, the DRHBc corrections are around 7.51 MeV, which are contributed by 6.05 MeV from the deformed intrinsic mean field and 1.91 MeV from the beyond mean-field effects.

The KRR corrections on the RCHB results are shown in Fig. 4(a), and the rms value is 8.33 MeV. By comparing the results in Figs. 3(a) and 4(a), it is found that the patterns of the corrections are similar, indicating that the KRR corrections are mainly contributed by the deformation effects. The remaining corrections after subtracting the intrinsic deformed mean-field corrections from DRHBc are shown in Fig. 4(b), with the rms value 2.85 MeV. A part of the contributions to the corrections is certainly attributed to the rotational
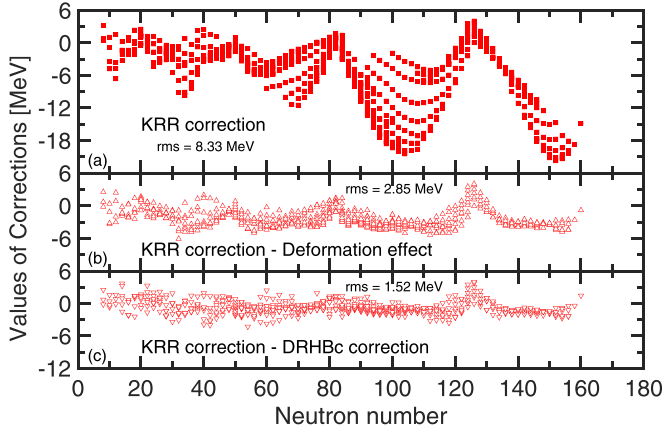
FIG. 4. (a) The KRR corrections on the RCHB predictions. (b) The differences between the KRR corrections and the intrinsic deformation effects in the DRHBc corrections. (c) The differences between the KRR corrections and the full DRHBc corrections.
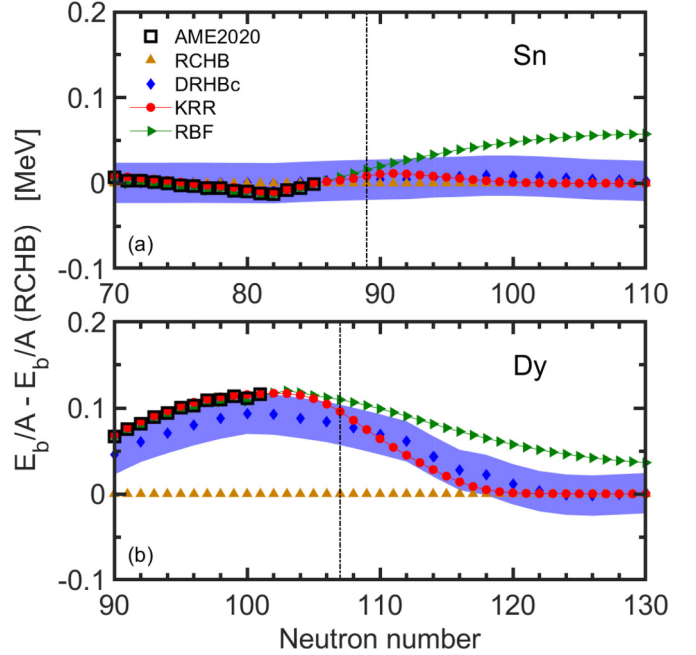

FIG. 5. The RCHB, DRHBc, KRR, RBF predictions and the experimental data for Sn (a) and Dy (b) isotopes. The values are subtracted with the RCHB predictions. The purple band represents the uncertainty of the nuclear masses of the DRHBc model, which is evaluated by the rms deviation from the experimental data. The vertical bar in each panel shows the last experimentally known nucleus [78].

corrections from the beyond mean-field effects for the deformed nuclei. The remaining corrections after further subtracting the rotational corrections are shown in Fig. 4(c), with the rms value 1.52 MeV. This part of corrections still exhibits slightly parabolic behavior in the regions between closed shells, which indicates that it still includes some deformation effects which are not fully included in the DRHBc theory, e.g., triaxiality [77]. Certainly, the remaining corrections should also include some other effects beyond the scope of the DRHBc theory, such as the beyond-mean-field vibrational corrections, the effects of the exchange interactions, etc.

The above discussions illustrate the accuracy of the refined RCHB predictions with the KRR corrections in reproducing experimentally known nuclear masses. It is also important to examine the reliability of the KRR corrections when extrapolated to the regions without mass data. According to the analysis above, the KRR corrections and the DRHBc corrections share large common contributions induced by the deformation effects. As the DRHBc corrections with deformation effects are the most important missing effects in the RCHB calculation, the DRHBc predictions can be regarded as good pseudoexperimental data. Therefore, we can take the opportunity to examine the reliability of the KRR corrections by comparing with the DRHBc predictions in the region without experimental mass data.

The performance of the KRR extrapolation had been examined to be reliable in the previous work [67], which shows that the KRR approach can avoid the risk of worsening the mass description for nuclei at large extrapolation distances. This holds true for the present cases. Here, we would take two typical isotopes, i.e., tin stands for spherical isotopes and dysprosium stands for deformed isotopes, to validate the extrapolation ability of the KRR corrections on the RCHB predictions. The comparison of the RCHB, DRHBc, and KRR mass predictions of tin and dysprosium isotopes are presented in Fig. 5. The experimental data AME2020, and the results from another machine-learning approach, the radial basis function (RBF) [68,79], are presented for comparison.

The setups of the learning procedure of the RBF approach, including the training and validation, are the same as the KRR approach adopted in the present work.

The tin isotopes with proton number $Z = 50$ are proton-magic nuclei, and most of them are spherical or near spherical. Therefore, the RCHB predictions are in good agreement with the experimental data, and the DRHBc predictions are similar with the RCHB ones. For the region with experimentally known masses, i.e., $N \leqslant 85$, both the KRR and RBF approaches can well reproduce the experimental data and the DRHBc predictions. However, when moving to the region without experimental data, the RBF predictions go far away from the RCHB predictions, while the KRR predictions still match with the RCHB predictions. Since most tin isotopes are expected to be spherical or near spherical, the KRR predictions that match with the RCHB predictions are more reliable. Another hint of the reliability of the KRR approach is that the KRR predictions still lie in the uncertainty band of the DRHBc predictions when moving to the region without experimental data. On the contrary, the RBF predictions run away from the uncertainty band when moving to the experimentally unknown region, although the RBF approach has achieved satisfactory accuracy in refining the RCHB mass predictions for experimentally known region [79].

The dysprosium isotopes, with proton number $Z = 66$ lying between magic numbers 50 and 82, are mostly well deformed. Therefore, the RCHB predictions significantly deviate from the experimental data. Note that the DRHBc

predictions also deviate from the experimental data, but the data still lie in the uncertainty band of the DRHBc predictions. For the region with experimentally known masses, i.e., $N \leqslant 101$, both the KRR and RBF approaches can well reproduce the experimental data and they all lie in the DRHBc uncertainty band. For the region without experimental data, the RBF predictions gradually deviate from the DRHBc uncertainty band, while the KRR predictions still lie in the DRHBc uncertainty band. Especially, when the extrapolations move to the regions where the neutron number is close to the magic number $N = 126$, the DRHBc predictions come back to the spherical RCHB predictions. This behavior is well reproduced only by the KRR approach. These examinations manifest the reliability of the KRR extrapolation in refining the RCHB predictions.

For both tin and dysprosium isotopes, one can see that the KRR predictions would return to the RCHB predictions when extrapolated to nuclei at large distances, e.g., ^{150}Sn for tin isotope and ^{186}Dy for dysprosium isotopes. This is because of the decay behavior of the Gaussian kernel with the increase of extrapolation distance. This behavior limits the KRR approach to extrapolate to large distances, but it also helps the KRR approach avoid the risk of worsening the mass description for nuclei at large extrapolation distances. The details of this behavior and the limit of the extrapolation distance in the KRR approach have been discussed in Ref. [67].

V. SUMMARY

In summary, the KRR approach and the RCHB mass model are combined to construct a high-precision and reliable nuclear mass model that can describe both stable and exotic nuclei. The refined RCHB predictions with KRR approach can achieve an accuracy of rms deviation 385 keV with the experimental masses. The KRR corrections on the RCHB masses are compared with the DRHBc corrections to analyze the physical effects included in the KRR corrections. It is found that the major contributions contained in the KRR corrections are from the deformation effects at the mean-field level, and the rotational corrections from the beyond mean-field effects also play an important role. Detailed comparisons also indicate that the KRR corrections contain some effects beyond the scope of the DRHBc theory, such as the triaxial deformation and vibrational corrections. The DRHBc predictions are taken as the pseudoexperimental data to examine the KRR extrapolations on nuclei without mass data. The examinations manifest very well the reliability of the extrapolation of the KRR approach in refining the RCHB predictions. For perspective, the KRR approach with odd-even effects (KRRoe) can be employed to further refine the RCHB predictions. This will be even more appealing in case the DRHBc mass table for odd-mass and odd-odd nuclei are also finished, so that we can use the data to analyze the odd-even effects in the KRRoe correction and validate the extrapolation performance for nuclei with different number parity of proton and neutron.

ACKNOWLEDGMENTS

[1] D. Lunney, J. M. Pearson, and C. Thibault, Rev. Mod. Phys. **75**, 1021 (2003).

[2] E. M. Burbidge, G. R. Burbidge, W. A. Fowler, and F. Hoyle, Rev. Mod. Phys. **29**, 547 (1957).

[3] A. de Roubin, D. Atanasov, K. Blaum, S. George, F. Herfurth, D. Kisler, M. Kowalska, S. Kreim, D. Lunney, V. Manea, E. Minaya Ramirez, M. Mougeot, D. Neidherr, M. Rosenbusch, L. Schweikhard, A. Welker, F. Wienholtz, R. N. Wolf, and K. Zuber, Phys. Rev. C **96**, 014310 (2017).

[4] E. M. Ramirez, D. Ackermann, K. Blaum, M. Block, C. Droese, C. E. Düllmann, M. Dworschak, M. Eibach, S. Eliseev, E. Haettner, F. Herfurth, F. P. Heßberger, S. Hofmann, J. Ketelaer, G. Marx, M. Mazzocco, D. Nesterenko, Y. N. Novikov, W. R. Plaß, D. Rodríguez *et al.*, Science **337**, 1207 (2012).

[5] F. Wienholtz, D. Beck, K. Blaum, C. Borgmann, M. Breitenfeldt, R. B. Cakirli, S. George, F. Herfurth, J. D. Holt, M. Kowalska, S. Kreim, D. Lunney, V. Manea, J. Menéndez, D. Neidherr, M. Rosenbusch, L. Schweikhard, A. Schwenk, J. Simonis, J. Stanja *et al.*, Nature (London) **498**, 346 (2013).

[6] H. A. Bethe, Phys. Rev. **55**, 434 (1939).

[7] M. R. Mumpower, R. Surman, G. C. McLaughlin, and A. Aprahamian, Prog. Part. Nucl. Phys. **86**, 86 (2016).

[8] X. F. Jiang, X. H. Wu, and P. W. Zhao, Astrophys. J. **915**, 29 (2021).

[9] X. H. Wu, P. W. Zhao, S. Q. Zhang, and J. Meng, Astrophys. J. **941**, 152 (2022).

[10] M. Wang, W. J. Huang, F. G. Kondev, G. Audi, and S. Naimi, Chin. Phys. C **45**, 030003 (2021).

[11] C. F. v. Weizsäcker, Z. Phys. **96**, 431 (1935).

[12] N. Wang, M. Liu, X. Wu, and J. Meng, Phys. Lett. B **734**, 215 (2014).

[13] P. Möller, A. J. Sierk, T. Ichikawa, and H. Sagawa, At. Data Nucl. Data Tables **109**, 1 (2016).

[14] H. Koura, T. Tachibana, M. Uno, and M. Yamada, Prog. Theor. Phys. **113**, 305 (2005).

[15] J. M. Pearson, R. C. Nayak, and S. Goriely, Phys. Lett. B **387**, 455 (1996).

[16] L. S. Geng, H. Toki, and J. Meng, Prog. Theor. Phys. **113**, 785 (2005).

[17] S. Goriely, N. Chamel, and J. M. Pearson, Phys. Rev. Lett. **102**, 152503 (2009).

[18] S. Goriely, S. Hilaire, M. Girod, and S. Péru, Phys. Rev. Lett. **102**, 242501 (2009).

[19] D. Peña-Arteaga, S. Goriely, and N. Chamel, Euro. Phys. J. A **52**, 320 (2016).

[20] X. W. Xia, Y. Lim, P. W. Zhao, H. Z. Liang, X. Y. Qu, Y. Chen, H. Liu, L. F. Zhang, S. Q. Zhang, Y. Kim, and J. Meng, At. Data Nucl. Data Tables **121**, 1 (2018).

[21] Y. L. Yang, Y. K. Wang, P. W. Zhao, and Z. P. Li, Phys. Rev. C **104**, 054312 (2021).

[22] K. Zhang, M.-K. Cheoun, Y.-B. Choi, P. S. Chong, J. Dong, Z. Dong, X. Du, L. Geng, E. Ha, X.-T. He, C. Heo, M. C. Ho, E. J. In, S. Kim, Y. Kim, C.-H. Lee, J. Lee, H. Li, Z. Li, T. Luo *et al.*, At. Data Nucl. Data Tables **144**, 101488 (2022).

[23] P. W. Zhao, L. S. Song, B. Sun, H. Geissel, and J. Meng, Phys. Rev. C **86**, 064324 (2012).

[24] K. Zhang, X. He, J. Meng, C. Pan, C. Shen, C. Wang, and S. Zhang, Phys. Rev. C **104**, L021301 (2021).

[25] J. Erler, N. Birge, M. Kortelainen, W. Nazarewicz, E. Olsen, A. M. Perhac, and M. Stoitsov, Nature (London) **486**, 509 (2012).

[26] Z. X. Ren and P. W. Zhao, Phys. Rev. C **102**, 021301(R) (2020).

[27] J. N. Ginocchio, Phys. Rev. Lett. **78**, 436 (1997).

[28] J. Meng, K. Sugawara-Tanabe, S. Yamaji, P. Ring, and A. Arima, Phys. Rev. C **58**, R628(R) (1998).

[29] T.-S. Chen, H.-F. Lü, J. Meng, S.-Q. Zhang, and S.-G. Zhou, Chin. Phys. Lett. **20**, 358 (2003).

[30] J. N. Ginocchio, Phys. Rep. **414**, 165 (2005).

[31] H. Liang, J. Meng, and S.-G. Zhou, Phys. Rep. **570**, 1 (2015).

[32] S.-G. Zhou, J. Meng, and P. Ring, Phys. Rev. Lett. **91**, 262501 (2003).

[33] X. T. He, S. G. Zhou, J. Meng, E. G. Zhao, and W. Scheid, Eur. Phys. J. A **28**, 265 (2006).

[34] W. Koepf and P. Ring, Nucl. Phys. A **493**, 61 (1989).

[35] J. König and P. Ring, Phys. Rev. Lett. **71**, 3079 (1993).

[36] P. W. Zhao, J. Peng, H. Z. Liang, P. Ring, and J. Meng, Phys. Rev. Lett. **107**, 122501 (2011).

[37] P. W. Zhao, N. Itagaki, and J. Meng, Phys. Rev. Lett. **115**, 022501 (2015).

[38] Y. K. Wang, Phys. Rev. C **97**, 064321 (2018).

[39] Z.-X. Ren, S.-Q. Zhang, P.-W. Zhao, N. Itagaki, J. A. Maruhn, and J. Meng, Sci. China Phys. Mech. Astron. **62**, 112062 (2019).

[40] Z. X. Ren, D. Vretenar, T. Nikšić, P. W. Zhao, J. Zhao, and J. Meng, Phys. Rev. Lett. **128**, 172501 (2022).

[41] K. Y. Zhang, P. Papakonstantinou, M.-H. Mun, Y. Kim, H. Yan, and X.-X. Sun, Phys. Rev. C **107**, L041303 (2023).

[42] K. Y. Zhang, S. Q. Yang, J. L. An, S. S. Zhang, P. Papakonstantinou, M.-H. Mun, Y. Kim, and H. Yan, Phys. Lett. B **844**, 138112 (2023).

[43] J. Zhao, B.-H. Sun, I. Tanihata, S. Terashima, A. Prochazka, J. Y. Xu, L. H. Zhu, J. Meng, J. Su, K. Zhang, L. S. Geng, L. C. He, C. Y. Liu, G. S. Li, C. G. Lu, W. J. Lin, W. P. Lin, Z. Liu, P. P. Ren, Z. Y. Sun *et al.*, Phys. Lett. B **847**, 138269 (2023).

[44] J. Meng and P. Ring, Phys. Rev. Lett. **77**, 3963 (1996).

[45] J. Meng, Nucl. Phys. A **635**, 3 (1998).

[46] J. Meng and P. Ring, Phys. Rev. Lett. **80**, 460 (1998).

[47] J. Meng, I. Tanihata, and S. Yamaji, Phys. Lett. B **419**, 1 (1998).

[48] J. Meng, S.-G. Zhou, and I. Tanihata, Phys. Lett. B **532**, 209 (2002).

[49] J. Meng, H. Toki, J. Y. Zeng, S. Q. Zhang, and S.-G. Zhou, Phys. Rev. C **65**, 041302(R) (2002).

[50] S.-Q. Zhang, J. Meng, S.-G. Zhou, and J.-Y. Zeng, Chin. Phys. Lett. **19**, 312 (2002).

[51] S. Zhang, J. Meng, and S. Zhou, Sci. China G **46**, 632 (2003).

[52] H. F. Lü, J. Meng, S. Q. Zhang, and S.-G. Zhou, Eur. Phys. J. A **17**, 19 (2003).

[53] W. Zhang, J. Meng, S. Q. Zhang, L. S. Geng, and H. Toki, Nucl. Phys. A **753**, 106 (2005).

[54] J. Meng, H. Toki, S. G. Zhou, S. Q. Zhang, W. H. Long, and L. S. Geng, Prog. Part. Nucl. Phys. **57**, 470 (2006).

[55] Y. Lim, X. Xia, and Y. Kim, Phys. Rev. C **93**, 014314 (2016).

[56] Y. Kuang, X. L. Tu, J. T. Zhang, K. Y. Zhang, and Z. P. Li, Euro. Phys. J. A **59**, 160 (2023).

[57] P. W. Zhao, Z. P. Li, J. M. Yao, and J. Meng, Phys. Rev. C **82**, 054319 (2010).

[58] S.-G. Zhou, J. Meng, P. Ring, and E.-G. Zhao, Phys. Rev. C **82**, 011301(R) (2010).

[59] L. Li, J. Meng, P. Ring, E.-G. Zhao, and S.-G. Zhou, Phys. Rev. C **85**, 024312 (2012).

[60] K. Zhang, M.-K. Cheoun, Y.-B. Choi, P. S. Chong, J. Dong, L. Geng, E. Ha, X. He, C. Heo, M. C. Ho, E. J. In, S. Kim, Y. Kim, C.-H. Lee, J. Lee, Z. Li, T. Luo, J. Meng, M.-H. Mun, Z. Niu *et al.* (DRHBc Mass Table Collaboration), Phys. Rev. C **102**, 024314 (2020).

[61] C. Pan, M.-K. Cheoun, Y.-B. Choi, J. Dong, X. Du, X.-H. Fan, W. Gao, L. Geng, E. Ha, X.-T. He, J. Huang, K. Huang, S. Kim, Y. Kim, C.-H. Lee, J. Lee, Z. Li, Z.-R. Liu, Y. Ma, J. Meng *et al.* (DRHBc Mass Table Collaboration), Phys. Rev. C **106**, 014316 (2022).

[62] DRHBc Mass Table Collaboration, http://drhbctable.jcnp.org/.

[63] G. Carleo, I. Cirac, K. Cranmer, L. Daudet, M. Schuld, N. Tishby, L. Vogt-Maranto, and L. Zdeborová, Rev. Mod. Phys. **91**, 045002 (2019).

[64] A. Boehnlein, M. Diefenthaler, N. Sato, M. Schram, V. Ziegler, C. Fanelli, M. Hjorth-Jensen, T. Horn, M. P. Kuchera, D. Lee, W. Nazarewicz, P. Ostroumov, K. Orginos, A. Poon, X.-N. Wang, A. Scheinker, M. S. Smith, and L.-G. Pang, Rev. Mod. Phys. **94**, 031003 (2022).

[65] W. He, Q. Li, Y. Ma, Z. Niu, J. Pei, and Y. Zhang, Sci. China-Phys. Mech. Astron. **66**, 282001 (2023).

[66] X. H. Wu, Z. X. Ren, and P. W. Zhao, Phys. Rev. C **105**, L031303 (2022).

[67] X. H. Wu and P. W. Zhao, Phys. Rev. C **101**, 051301(R) (2020).

[68] Z. M. Niu, Z. L. Zhu, Y. F. Niu, B. H. Sun, T. H. Heng, and J. Y. Guo, Phys. Rev. C **88**, 024325 (2013).

[69] Z. M. Niu and H. Z. Liang, Phys. Lett. B **778**, 48 (2018).

[70] L. Neufcourt, Y. C. Cao, W. Nazarewicz, and F. Viens, Phys. Rev. C **98**, 034318 (2018).

[71] Z. M. Niu and H. Z. Liang, Phys. Rev. C **106**, L021303 (2022).

[72] X. H. Wu, L. H. Guo, and P. W. Zhao, Phys. Lett. B **819**, 136387 (2021).

[73] X. H. Wu, Y. Y. Lu, and P. W. Zhao, Phys. Lett. B **834**, 137394 (2022).

[74] L. H. Guo, X. H. Wu, and P. W. Zhao, Symmetry **14**, 1078 (2022).

[75] X. H. Wu, Front. Phys. **11**, 1061042 (2023).

[76] X.-K. Du, P. Guo, X.-H. Wu, and S.-Q. Zhang, Chin. Phys. C **47**, 074108 (2023).

[77] K. Y. Zhang, S. Q. Zhang, and J. Meng, Phys. Rev. C **108**, L041301 (2023).

[78] National Nuclear Data Center (NNDC), https://www.nndc.bnl.gov/.

[79] M. Shi, Z.-M. Niu, and H.-Z. Liang, Chin. Phys. C **43**, 074104 (2019).